ELSEVIER

Biophysical Chemistry 114 (2005) 235–244

Biophysical Chemistry

http://www.elsevier.com/locate/biophyschem

Kinetic studies of iron deposition catalyzed by recombinant human liver heavy, and light ferritins and *Azotobacter vinelandii* bacterioferritin using O_2 and H_2O_2 as oxidants

Jared Bunker[a], Thomas Lowry[a], Garrett Davis[a], Bo Zhang[b], David Brosnahan[b], Stuart Lindsay[b], Robert Costen[c], Sang Choi[c], Paolo Arosio[d], Gerald D. Watt[b,*]

[a]*Brigham Young University Undergraduate Research Program, United States*
[b]*Department of Chemistry and Biochemistry, Brigham Young University, Provo, Utah 84602, United States*
[c]*The NASA Langley Research Center, Hampton, VA 23681, United States*
[d]*Unit of Protein Engineering, DIBIT, San Raffaele Scientific Institute, Milano and Cattedra di Chimica, University of Brescia, Brescia, Italy*

Received 10 June 2004; received in revised form 19 September 2004; accepted 16 November 2004
Available online 7 January 2005

Abstract

The discrepancy between predicted and measured H_2O_2 formation during iron deposition with recombinant heavy human liver ferritin (rHF) was attributed to reaction with the iron protein complex [Biochemistry 40 (2001) 10832–10838]. This proposal was examined by stopped-flow kinetic studies and analysis for H_2O_2 production using (1) rHF, and *Azotobacter vinelandii* bacterial ferritin (AvBF), each containing 24 identical subunits with ferroxidase centers; (2) site-altered rHF mutants with functional and dysfunctional ferroxidase centers; and (3) recombinant human liver light ferritin (rLF), containing no ferroxidase center. For rHF, nearly identical pseudo-first-order rate constants of 0.18 s^{-1} at pH 7.5 were measured for Fe^{2+} oxidation by both O_2 and H_2O_2, but for rLF, the rate with O_2 was 200-fold slower than that for H_2O_2 (k=0.22 s^{-1}). A Fe^{2+}/O_2 stoichiometry near 2.4 was measured for rHF and its site altered forms, suggesting formation of H_2O_2. Direct measurements revealed no H_2O_2 free in solution 0.5–10 min after all Fe^{2+} was oxidized at pH 6.5 or 7.5. These results are consistent with initial H_2O_2 formation, which rapidly reacts in a secondary reaction with unidentified solution components. Using measured rate constants for rHF, simulations showed that steady-state H_2O_2 concentrations peaked at 14 μM at ~600 ms and decreased to zero at 10–30 s. rLF did not produce measurable H_2O_2 but apparently conducted the secondary reaction with H_2O_2. Fe^{2+}/O_2 values of 4.0 were measured for AvBF. Stopped-flow measurements with AvBF showed that both H_2O_2 and O_2 react at the same rate (k=0.34 s^{-1}), that is faster than the reactions with rHF. Simulations suggest that AvBF reduces O_2 directly to H_2O without intermediate H_2O_2 formation.

Keywords: Hydrogen peroxide; Human liver ferritin; Bacterioferritin; Iron deposition; Recombinant ferritins; Kinetics

1. Introduction

Ferritins are hollow, 24-subunit proteins involved in cellular iron storage, regulation, and detoxification [1–5]. Up to 4500 iron atoms are stored within the ~8.0 nm hollow ferritin interior in the form of hydrous iron (III) oxy-hydroxide mineral cores, whose surface is covered with a phosphate layer in animal ferritins [6,7] or as a homogeneous phospho-oxy-hydroxide mineral core in bacterioferritins [8,9]. Besides the difference in the chemical make-up of the mineral cores, the protein subunit composition between animal and bacterioferritin also differs [3,10]. Bacterioferritins are composed of a single subunit type (M_r~19000), with each subunit possessing a ferroxidase center related to that in animal ferritins, whereas, animal ferritins typically contain two different but similar types of subunits: heavy (H) and light (L). The H subunit contains a ferroxidase center that catalyzes Fe^{2+} oxidation by O_2, while

* Corresponding author. Tel.: +1 801 378 4561; fax: +1 801 378 5474.
E-mail address: gdwatt@chem.byu.edu (G.D. Watt).

0301-4622/$ - see front matter © 2004 Elsevier B.V. All rights reserved.
doi:10.1016/j.bpc.2004.11.008

the L subunit, without a ferroxidase center, still catalyzes Fe^{2+} oxidation but at a much slower rate [11–13].

The in vitro reaction of native apo horse spleen ferritin and recombinant heavy ferritins with Fe^{2+} and O_2 readily produces reconstituted mineral cores. Extensive kinetic and stoichiometric studies have proposed that two limiting Fe^{2+}/O_2 stoichiometries [14–17] occur during ferritin core reconstitution as summarized by Reactions (1) and (2).

$$2Fe^{2+} + O_2 + 6H_2O = 2Fe(OH)_3 + H_2O_2 + 4H^+ \quad (1)$$

$$4Fe^{2+} + O_2 + 10H_2O = 4Fe(OH)_3 + 8H^+ \quad (2)$$

Fe^{2+}/O_2 values near 2.0 at low iron loading levels suggest the formation of H_2O_2 by Reaction (1), and values near 4.0 at high iron loading levels suggest reduction of O_2 to H_2O by Reaction (2) [14,16,17]. From these results, it was proposed that the ferroxidase centers in native and recombinant heavy ferritins initially catalyze Reaction (1) but then Reaction (2) becomes important after a sufficiently large mineral core forms.

Different behavior from that occurring with animal ferritins was reported for the heme-containing bacterioferritins. Iron deposition with O_2 in *Escherichia coli* bacterioferritin (EcBF)[1], which consists of 24 H-like subunits containing a ferroxidase center similar to that in animal ferritins, does not form H_2O_2 but instead forms H_2O [18]. Similarly, *Listeria innocua* ferritin (LiBF), composed of only 12 subunits produces only H_2O [19]. These distinct differences in O_2 reactivity are remarkable, and it was suggested that the ferroxidase centers of animal and bacterioferritins, although similar, were different enough to explain this different reactivity [18]. This unusual difference deserves additional clarification to better define the reactivity at the ferroxidase site and determine how O_2 reactivity is influenced by small differences in the ferroxidase site.

We recently investigated the iron deposition reaction in HoSF and did not detect formation of H_2O_2 with changes in conditions [20]. To explain its absence, several reactions of H_2O_2 with the HoSF protein shell or the mineral core were considered, but chemically relevant reactions consistent with available information were difficult to formulate [20]. An independent follow-up study reported only 14% of the amounts of H_2O_2 predicted by Reaction (1) for HoSF, but values of 30–50% were previously reported for recombinant proteins [16,21]. To explain these smaller than predicted amounts of H_2O_2 by Reaction (1), the proposal was made that H_2O_2 rapidly reacted with the iron protein complex, thereby preventing its detection [21,22]. The rapid formation of H_2O_2 within 70 ms using recombinant frog H ferritin confirmed that H_2O_2 is an initial product of Fe^{2+} oxidation by O_2, but then its concentration rapidly decreases to near zero at ~30 s [23]. The loss of H_2O_2 with frog ferritin was also explained by a reaction with a secondary, unidentified system component. Similar results were reported for recombinant heavy human liver ferritin (rHF) [24,25] with maximum H_2O_2 formation occurring within 50–200 ms.

Recent kinetic studies with HoSF at low iron levels found that this secondary reaction with H_2O_2 was very rapid and occurred more quickly than the reaction of H_2O_2 with Fe^{2+} [26,27]. At higher iron loadings for both rHF and HoSF, different reactivity conditions prevail [28], as this secondary reaction is apparently suppressed or eliminated in favor of H_2O_2 reacting directly with Fe^{2+}, giving Fe^{2+}/O_2 values approaching 4.0 [17,21,28]. We report here the kinetics of the iron deposition reaction using rHF, site-altered rHF species and recombinant human liver light ferritin (rLF) at low iron loadings under similar conditions to compare with results for HoSF that is a heteropolymer composed of 4 H and 20 L subunit. Similar reactions using *Azotobacter vinelandii* bacterial ferritin (AvBF) were conducted to determine if O_2 is reduced to H_2O without the secondary reaction occurring as reported for EcBF and LiBF [18,19]. Using direct methods for H_2O_2 detection, stopped-flow kinetic measurements and kinetic simulations with various recombinant proteins, we report that for 2–5 μM rHF, H_2O_2 is present only at a steady-state concentration of ~14 μM at <1.0 s and decays rapidly to near zero at 10 s. These results show that H_2O_2 is only a transient product of O_2 reduction, because it has reacted further by a secondary reaction as previously proposed [21,23].

2. Materials and methods

rHF, its site-altered mutants, and rLF were provided by Dr. Paolo Arosio, and methods for their production and purification are described [29,30]. Site-altered rHFs have the following modifications: Cys 90 replaced by Glu (C90E), Trp 93 replaced by Phe (W93F), and the ferroxidase center amino acid ligands Glu 86 and His 65 replaced by Lys and Gly (222), respectively. These amino acid substitutions were chosen because (1) Cys 90 is on the exterior opening of the threefold channel and could be involved in iron entry into this channel; (2) Trp 93 is highly conserved and is implicated in redox reactions involving the protein shell [31]; and (3) 222 has the ferroxidase center of rHF modified to behave as rLF. Triply crystallized AvBF was prepared as previously described [31,32]. Small iron cores in the recombinant ferritins and AvBF were removed by reduction with dithionite and chelation with 2, 2′-bipyridine (bipy). Protein concentrations were determined by the Lowery method, with bovine serum albumin as standard. Fe^{2+} solutions were prepared at 16.0 mM using $FeSO_4 \cdot 7H_2O$ at pH~3. All air sensitive reactions were

[1] The abbreviations used are rHF, recombinant human liver heavy ferritin; rLF, recombinant human liver light ferritin; HoSF, horse spleen ferritin; AvBF, a BFR ferritin containing 12 heme groups isolated from *Azotobacter vinelandii*; EcBF, *Escherichia coli* bacterioferritin; LiBF, *Listeria innocua* bacterial ferritin. Site-altered rHFs have the following modifications: Cys 90 replaced by Glu (C90E), Trp 93 replaced by Phe (W93F). For rHF, Glu 86 and His 65 are replaced by Lys and Gly to form the rHF variant 222.

conducted in Vacuum Atmospheres glove boxes under N_2 with <0.1 ppm O_2 (Nyad Oxygen Monitor).

2.1. H_2O_2 measurements

The Amplex Red™ fluorometric procedure [20] was used to measure H_2O_2 formation in the presence of various ferritins, but only after all Fe^{2+} was consumed as evidenced by the kinetic reactions discussed below.

The Amplex Red reaction was also conducted anaerobically in the presence of Fe^{2+} but in the absence of ferritins by adding 1–100 μM Fe^{2+} to 1.0 mL portions of anaerobic 0.050 M Mops, 0.050 M NaCl at pH 7.5 and measuring the fluorometric response at 590 nm. The reaction was repeated with 1.0 mM EDTA present to evaluate the ability of EDTA to diminish the Amplex Red response to free Fe^{2+}. Anaerobic conditions were maintained to prevent Fe^{2+} oxidation by O_2 with possible formation of H_2O_2.

The Fe^{2+}/O_2 ratio for various ferritins was determined by the following procedures.

2.2. Chemical titrations with O_2

A series of 1.0 mL ferritin samples (~5 μM) in 0.05 M Mops, 0.05 M NaCl at pH 7.5 were made anaerobic in a glove box at Fe^{2+}/ferritin ratios of 10–50, O_2 (as an air-saturated solution at 210 μM in O_2) was added by gas-tight syringe, and the reaction mixture stirred for 10–30 min to ensure complete reaction. Unreacted Fe^{2+} was measured at 520 nm (ε=8400 $M^{-1}cm^{-1}$) after adding excess bipy to form $[Fe(bipy)_3]^{2+}$. The Fe^{2+}/O_2 ratio was varied from 10 to 1 to provide a wide titration range to evaluate the Fe^{2+}/O_2 reaction stoichiometry.

2.3. O_2 consumption measurements

O_2 uptake was measured directly using an Ocean Optics O_2 Fluorescence detector consisting of a FOXY-R Teflon-coated probe, LS-450 Blue LED Pulsed Light Source and an USB2000-FL spectrometer. Using air-saturated buffer solutions of 210 μM, a standard curve for the probe's response was created, demonstrating reliability to ~0.80 μM O_2. For Fe^{2+}/O_2 measurements, 2.0 mL of 1.0–5.0 μM ferritin was placed in an enclosed cell at a known dissolved O_2 concentration and continually stirred. Aliquots of 16.0 mM Fe^{2+} were added with a gas-tight syringe to react with all or a portion of the O_2 present. O_2 uptake measurements were also conducted by oximetry using a YSI Clark electrode as previously described [16,17].

2.4. Stopped-flow and pumped-flow kinetic measurements

Kinetic studies of Fe^{2+} oxidation with the various ferritins were conducted in 0.025 M Mops, 0.05 M NaCl at pH 6.5 and 7.5 with both H_2O_2 and O_2 as oxidants and analyzed as previously described [27]. Simulations were conducted as previously described [27].

3. Results

3.1. Iron deposition with rHF

Fig. 1 shows a series of 12 sequential additions of 10 Fe^{2+} to rHF and W93F at pH 7.5 with an O_2 concentration of 210 μM O_2. The absorbance change at 375 nm measures the rate of $Fe(OH)_3$ formation within the ferritin interior and shows that nearly identical absorbance changes occur for each incremental oxidation of Fe^{2+} to $Fe(OH)_3$. Similar reaction steps were observed for C90E but are not shown. The figure shows that no secondary slow reactions occur, and the reaction is complete in <30 s. Fe^{2+}/O_2 measurements gave values for rHF (2.4), C90E (2.5), and W93F (2.3) in agreement with previous results and are consistent with significant H_2O_2 formation [17,21].

Fig. 2 shows stopped-flow traces monitored at 375 nm for the oxidation of 50 Fe^{2+} using both O_2 (lower curve) and H_2O_2 (upper curve) at pH 7.5 and gives further details of the reactions shown in Fig. 1. The kinetic curves for rHF were best fit by two exponential functions (k1=0.18 s^{-1} and k2=0.04 s^{-1}) in Fe^{2+}. Nearly identical sets of rate constants for rHF at pH 7.5 were observed for both O_2 and H_2O_2. With H_2O_2, the absorbance change was ~15% higher than with O_2, and the kinetic profile showed a slightly slower rate after 4–5 s due to a greater contribution of k2. The iron deposition reactions with rHF are essentially identical using O_2 and H_2O_2 at pH 7.5 and with H_2O_2 at pH 6.5. However, the reaction with O_2 at pH 6.5 is approximately twofold slower than with H_2O_2, suggesting that the reaction of O_2 at the ferroxidase center possibly occurs by a different pH-sensitive process. Identical results to rHF were obtained for W93F but are not shown. When the same reaction was conducted with C90E using O_2 and H_2O_2 at pH 6.5 and 7.5, k1 (0.34 s^{-1}) was found to be approximately two times faster for both oxidants than corresponding reactions for rHF or W93F, and the reaction was 1.4 not twofold slower

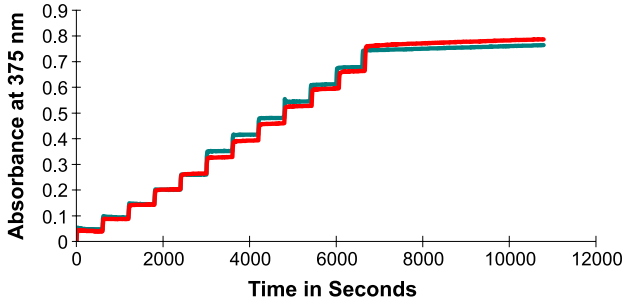

Fig. 1. Iron deposition monitored at 375 nm for 12 consecutive additions of 10 Fe^{2+} to rHF and W93F in 0.025 M Mops, 0.10 M NaCl at pH 7.5. Each addition was 3.0 μL of 16.3 mM $FeSO_4$ to 2.2 mL of 2.2 μM rHF and W93F. Both curves are superimposed for the first five additions, but after the sixth addition, the W93F had a slightly higher absorbance change.

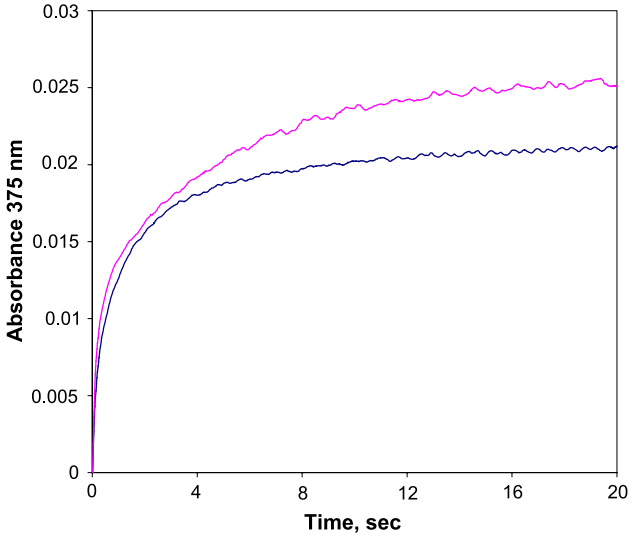

Fig. 2. The absorbance change at 375 nm measured by stopped-flow spectrophotometry for the addition of 45 μM Fe^{2+} to 0.94 μM rHF containing 210 μM O_2 (bottom curve), giving a final O_2 concentration of 105 μM. An identical reaction was conducted, except 210 μM H_2O_2 was present with the rHF solution which gave a final H_2O_2 concentration of 105 μM (upper curve). In both cases, the buffer was 0.025 M Mops, 0.10 M NaCl at pH 7.5.

with O_2 at pH 6.5. Both oxidants gave a slightly higher absorbance change for C90E and a greater contribution from k2 (0.05 s^{-1}). The rate constants for the iron deposition reactions with recombinant heavy ferritins are summarized in Table 1 and demonstrate that iron deposition with rHF and its variants is complete in <30 s and that unreacted Fe^{2+} is absent after this time interval. This result is important for the stoichiometric measurements discussed next, because unreacted Fe^{2+} can give a false positive response for H_2O_2 formation as previously described [20] and discussed later.

Fig. 3 shows the amount of H_2O_2 produced after 2.0 min for various recombinant ferritins and selected variants relative to control reactions measured by the Amplex Red fluorometric method. H_2O_2 was also measured at 30 s and 10.0 min and were identical to the results in Fig. 3. Similar low amounts of H_2O_2 were observed at pH 6.5 at 2.0 and 10 min, but analysis was not conducted at 30 s because the twofold slower reaction at this pH resulted in some unreacted Fe^{2+} that could interfere with the measurement of H_2O_2 (see later). These results demonstrate that H_2O_2 is

Table 1
Summary of rate constants determined by stopped-flow spectrophotometry for the O_2 and H_2O_2 reactions with various ferritins

Ferritin	pH	kO_2 (s^{-1})	kH_2O_2 (s^{-1})
rHF	7.5	0.18±0.03	0.17±0.03
rHF	6.5	0.084±0.05	0.17±0.04
C90E	7.5	0.34±0.03	0.43±0.03
W93F	7.5	0.17±0.02	0.24±0.03
rLF	7.5	0.0012	0.22±0.02
AvBF	7.5	0.42±0.03	0.44±0.03

The rate constants were obtained at 25 °C in 0.025 M Mops, 0.05 M NaCl, pH 7.5 at protein concentrations 2–5 μM.

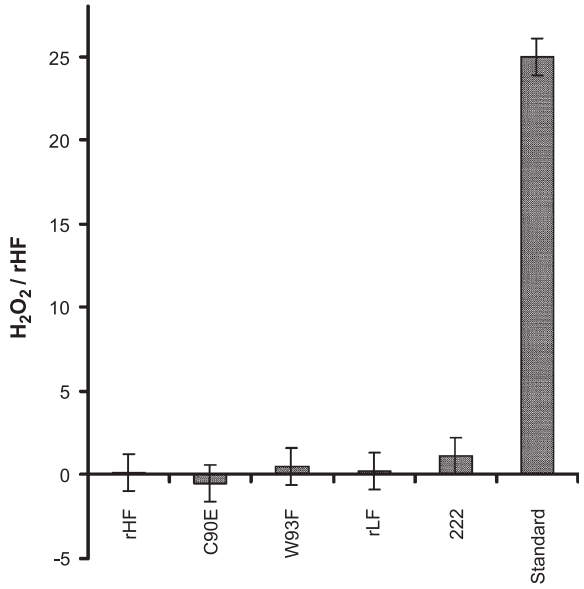

Fig. 3. H_2O_2 measured by fluorometry at 590 nm at pH 7.5 using Amplex Red 30 s after the addition of 50 Fe^{2+}/ferritin to 5 μM apo ferritin in 0.025 M Mops, 0.05 M NaCl at pH 7.5 containing 210 μM O_2. The first three bars represent peroxide detected from Fe^{2+} oxidation by rHF, C90E, and W93F that have functional ferroxidase centers. The positive control on the far right (Standard) predicts the response if all H_2O_2 in Reaction (1) remained in solution. rLF and 222 are negative controls: rLF does not possess a ferroxidase center; and 222 is an rHF mutant with a dysfunctional ferroxidase center.

at best only a minor product after 0.50–10 min (pH 7.5) and after 1–10 min (pH 6.5) using rHF or its site-altered forms with intact ferroxidase centers. The results suggest that H_2O_2 is formed but is rapidly consumed by a secondary reaction as proposed [21].

3.2. The iron deposition reaction with rLF

Fig. 4 compares the rate of deposition of 25 Fe^{2+} conducted with rLF at pH 7.5 with O_2 and H_2O_2 as oxidants

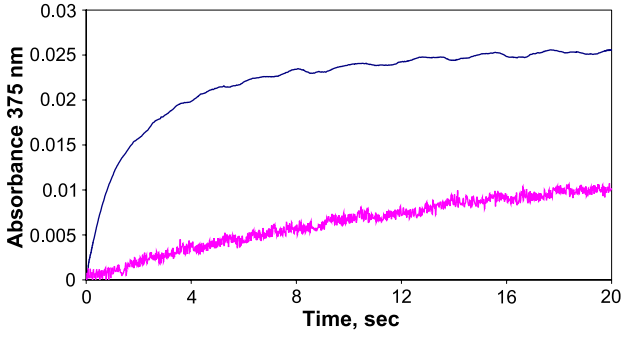

Fig. 4. The absorbance change at 375 nm monitored by stopped-flow spectrophotometry after addition of 45 μM Fe^{2+} to 1.8 μM rLF containing 0.025 M Mops, 0.05 M NaCl at pH 7.5, and 210 μM O_2 (bottom curve), giving a final O_2 concentration after mixing of 105 μM. An identical reaction was conducted, except 210 μM H_2O_2 was used giving a final concentration of 105 μM (upper curve).

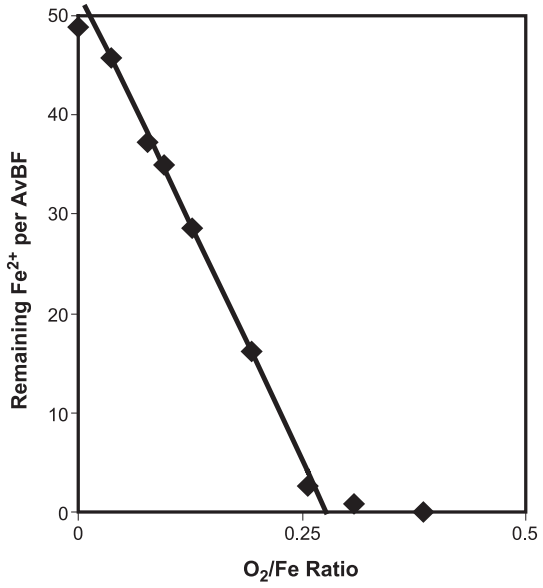

Fig. 5. Anaerobic titration of AvBF at 5.0 μM at a Fe^{2+}/AvBF ratio of 50 in 0.025 M Mops, 0.05 M NaCl at pH 7.5 with O_2. After a 10–30 min reaction time, excess α,α-bipyridine was added, and unreacted Fe^{2+} was determined as $[Fe(bipy)_3]^{2+}$ at 520 nm (ε=8400 $M^{-1}cm^{-1}$). Each point represents the result from an individual reaction vial in which a different amount of O_2 was added by a gas-tight syringe from an air-saturated solution (O_2=210 μM). All iron was oxidized as evidenced by the absence of $[Fe(bipy)_3]^{2+}$ at O_2/Fe ratios above 0.25 (Fe^{2+}/O_2=4.0).

and shows that Fe^{2+} oxidation is ~200 times faster with H_2O_2 (k=0.22 s^{-1}) than with O_2 (k ~0.0012 s^{-1}). For the addition of 500 Fe^{2+}, rLF was reported to react 100 times faster with H_2O_2 than O_2 [28]. This difference in rate could indicate that Fe^{2+} oxidation is sensitive to the amount of Fe^{2+} being processed, but in both cases, the rate is much faster with H_2O_2. These results demonstrate the effectiveness of the ferroxidase center in catalyzing the reaction with O_2 and also show that the rate of iron deposition with rLF and H_2O_2 at pH 7.5 occurs at a rate comparable to rHF (Table 1). Fe^{2+}/O_2 values of 2.65±0.35 were reported [28] for Fe^{2+} oxidation by O_2 with rLF, indicating that H_2O_2 is initially formed by rLF and rapidly and quantitatively reacts in a secondary reaction as proposed for rHF because no H_2O_2 is detected. This result suggests that the secondary reaction must occur at a site other than the ferroxidase center, which is lacking in rLF.

3.3. Reactions with catalase

The Fe^{2+}/O_2 ratio for rHF and rLF changes from ~2.5 to ~4.0 in the absence and presence of catalase [16,17,21,28], respectively, suggesting that free H_2O_2 is initially formed and decomposed by catalase. Stopped-flow kinetic measurements for rHF and rLF at 5.0 μM at pH 7.5 in 210 μM O_2 were run in the presence and absence of 2.0 μM catalase, but no difference in the lower curves in both Figs. 2 and 4 was found. This behavior is different from the corresponding reaction with HoSF, where catalase slowed the O_2 reaction 1.5-fold but only for the initial oxidation step [27].

3.4. AvBF reactions

Fig. 5 is an O_2 titration of anaerobic AvBF containing 50 Fe^{2+}/AvBF (~2.0 Fe^{2+}/ferroxidase center), to which excess bipy was added after 2–30 min to determine the amount of unreacted Fe^{2+}. For several additions, the Fe^{2+} concentration decreased linearly to zero at an O_2/Fe^{2+} ratio of 0.25±0.015 (Fe^{2+}/O_2=4.0±0.18), indicating the reduction of O_2 to H_2O. AvBF as isolated contains phosphate and iron at a 1:1 ratio within the core but can be reconstituted to form a phosphate-free $Fe(OH)_3$ mineral core. It was of interest to compare the Fe^{2+}/O_2 stoichiometry for formation of phosphate-containing and phosphate-free mineral cores in AvBF. Both oximetry and O_2 titration measurements gave values of 3.8 and 4.0 in the presence and absence of 10.0 mM phosphate, demonstrating that the Fe^{2+}/O_2 stoichiometry is independent of the core type being formed and that O_2 is reduced to H_2O.

Additional iron deposition reactions were conducted at pH 7.5 with AvBF using both O_2 and H_2O_2 at 50 Fe/AvBF, both in the absence and in the presence of 10.0 mM phosphate, and similar results (not shown) to Figs. 1 and 2 were observed and reported in Table 1. As with rHF, identical rates were found for iron deposition using either O_2 or H_2O_2, but AvBF reacts ~1.3 times faster than the C90E and ~2.5 times faster than rHF. H_2O_2 measurements were conducted when all Fe^{2+} was completely reacted, and Fig. 6 shows that no H_2O_2 was observed within 30 s of Fe^{2+} addition either in the presence or in the absence of phosphate. The same results were found under O_2-limiting conditions or at pH 6.5. The results in Figs. 5 and 6 establish that O_2 is reduced to H_2O, but the identical rates for the O_2 and H_2O_2 reactions, and the large excess of O_2 present in the reaction (210 μM), compared to the much smaller amount of

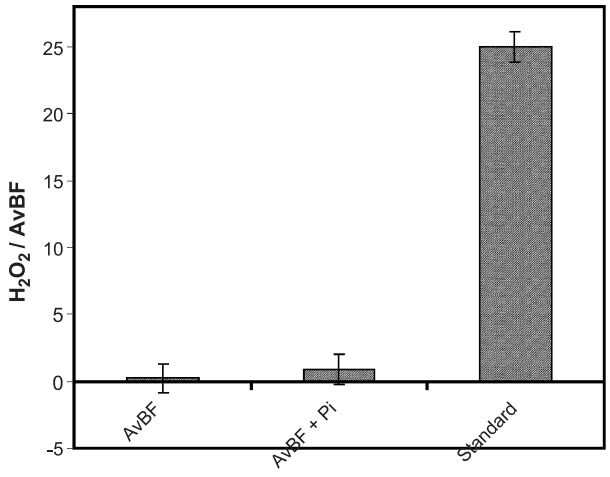

Fig. 6. H_2O_2 measured following iron deposition with AvBF under conditions similar to Fig. 1. The AvBF concentration was 5.0 μM in 0.025 M Mops, 0.05M NaCl at pH 7.5 at a Fe^{2+}/AvBF ratio of 50. An identical reaction was conducted in the presence of 1.0 mM phosphate. A standard addition of H_2O_2 according to Reaction (1) is shown as the entry on the right (Standard).

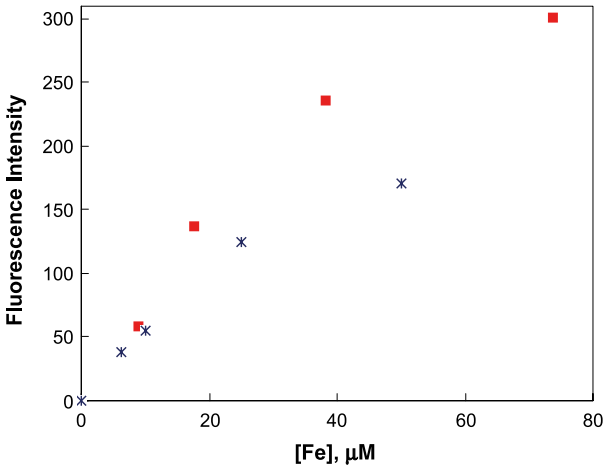

Fig. 7. The fluorescence response recorded under anaerobic conditions at 590 nm as a function of Fe^{2+} concentration for the reaction of Fe^{2+} with the Amplex Red reagents in 0.025 M Mops, 0.05M NaCl at pH 7.5 in the absence (■) and presence of 1.0 mM EDTA (∗). The fluoresence response produced by 80 μM Fe^{2+}corresponds to about 10 μM H_2O_2.

H_2O_2 that could be expected, require that iron deposition occurs by O_2 reduction to H_2O, a result consistent with later kinetic simulations.

3.5. Amplex red reactions

We initially reported that Fe^{2+} gives a false positive response for H_2O_2 using Amplex Red and that addition of EDTA decreased this interference [20]. The upper data points in Fig. 7 show that Fe^{2+}causes a strong response at 590 nm under anaerobic conditions. EDTA diminishes the effect but in a concentration-dependent manner. At Fe^{2+} concentrations below 10 μM, the effect of adding EDTA is small, but at higher concentrations, it lowers but does not eliminate the response of Fe^{2+} with Amplex Red. Our initial observation that EDTA decreases the response was not conducted over a wide enough Fe^{2+} concentration range to see the entire effect and, as we now report, EDTA has only a weakly ameliorating effect at high Fe^{2+} concentrations. This behavior indicates that addition of the Amplex Red reagents to ferritin solutions that contain unreacted Fe^{2+} can create an elevated fluorescence reading and give an apparently higher H_2O_2 level than is actually formed, even in the presence of EDTA. It is important to add the reagents after the reaction have consumed all Fe^{2+} in order to avoid a false positive response. Figs. 1 and 2 show that Fe^{2+} oxidation is complete within 30 s, hence H_2O_2 measurements with Amplex Red after this time interval (Fig. 3) should be free from interference by unreacted Fe^{2+}.

4. Discussion

Extensive stoichiometric measurements with animal ferritins and their variants at low iron loadings of 10–100 Fe/ferritin give Fe^{2+}/O_2 values of 2.0–2.5 that suggest H_2O_2 is an initial product of iron deposition with O_2 [14,16,17,21,28]. However, direct H_2O_2 measurements showed it did not accumulate in solution [20] or accumulated only to a low level [21]. This discrepancy was explained [21,23] by assuming the newly formed H_2O_2 reacted rapidly in a secondary reaction with the iron protein complex. This proposal is also consistent with measurements conducted in the presence of catalase that gave stoichiometric values near 4.0, presumably by decomposing the H_2O_2 before the secondary reaction occurs. Stopped-flow measurements for the iron deposition reaction for HoSF using O_2 and H_2O_2 and kinetic simulations were consistent with this interpretation and showed [27] that this secondary reaction was ~10 times faster with H_2O_2 and out-competed Fe^{2+} oxidation for the newly formed H_2O_2. The simulations for HoSF predicted Fe^{2+}/O_2 values of ~2.5, peak steady-state levels of H_2O_2 of 0.40 μM after 1–5 s, and the absence of H_2O_2 after Fe^{2+} oxidation (>100 s), because all H_2O_2 free in solution was consumed by the secondary reaction.

Similar Fe^{2+}/O_2 values of ~2.5 and 4.0 were reported for rHF by oximetric measurements in the absence and presence of catalase [15–17], implying nearly complete H_2O_2 formation. The lower Fe^{2+}/O_2 value for rHF was also explained by a secondary reaction consuming all H_2O_2 to yield values near 2.0–2.5 and not 4.0 [21,28]. However, this explanation is not as straightforward as in the case of HoSF, because for rHF, 30–50% of the H_2O_2 predicted by Reaction (1) was released as O_2 when catalase was added following the iron deposition reaction. This result is difficult to reconcile with the proposal that *all* H_2O_2 is consumed in a secondary reaction to produce a Fe^{2+}/O_2 value near 2.0.

This complexity is even more pronounced with frog H ferritin, because recent results [23] show an initial quantitative formation of H_2O_2 by Reaction (1) within 70 ms, whose concentration decreases to zero at 30 s due to a secondary reaction. This result predicts H_2O_2 would be absent, and no O_2 should be produced by catalase, a prediction inconsistent with the earlier measurement of 30–50% O_2 release for this same protein [16]. The reaction with these recombinant proteins appears to be more complex than that with HoSF and possibly prone to reactions from more than one pathway.

The Fe^{2+}/O_2 stoichiometry for rLF is relevant to the secondary reaction of H_2O_2 after its formation, because values of 2.7±0.1 and 2.65±0.35 (3.42±0.17 in the presence of catalase) were reported in the absence of catalase, respectively [15,28]. These values suggest initial H_2O_2 formation that reacts in a secondary reaction, because

$$2\,Fe^{2+} + O_2 + 6H_2O = 2Fe(OH)_3 + H_2O_2 + 4H^+ \quad (1)$$

$$\underline{H_2O_2 + X = XO + H_2O} \quad (3)$$

$$2Fe^{2+} + O_2 + 5H_2O + X = 2Fe(OH)_3 + XO + 4H^+ \quad (4)$$

Scheme 1.

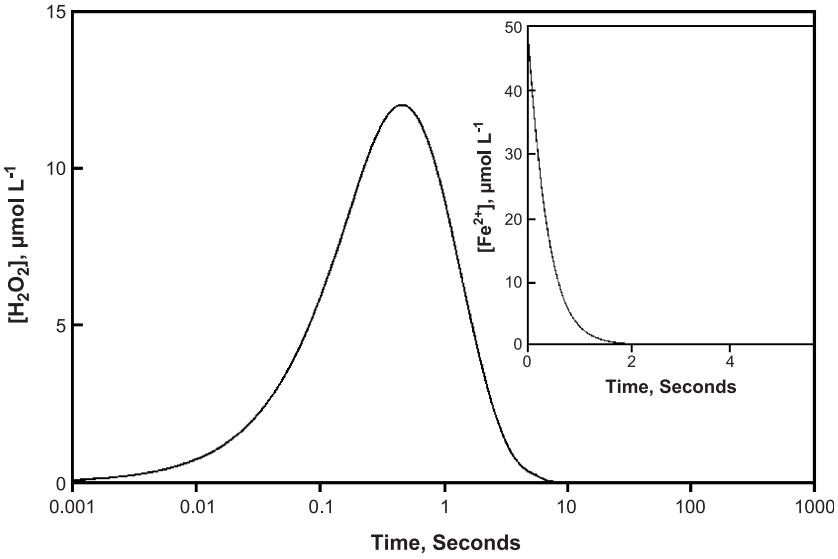

Fig. 8. Simulation of H_2O_2 production as a function of time at pH 7.5 and 5.0 μM rHF at a Fe^{2+}/rHF ratio of 50 using the rate constant of 0.18 s^{-1} in Table 1 applied to Scheme 1. The inset is the simulation of Fe^{2+} concentration decreasing as a function of time. The differential equations and the mathematical procedure were previously described [27].

Fig. 3 shows that H_2O_2 is not detectable for the iron deposition reaction using rLF. The rate constant for the secondary reaction with rLF also must be >10 times that for the reaction of Fe^{2+} with H_2O_2 to give measured Fe^{2+}/O_2 values of ~2.7.

In order to gain an understanding of (1) the iron oxidation reaction using O_2 with recombinant ferritins, (2) the formation of H_2O_2 by homopolymeric recombinant human liver proteins, and (3) the rapid secondary reaction between the newly formed H_2O_2 and the ferritin system component, we conducted kinetic, Fe^{2+}/O_2 stoichiometric measurements and H_2O_2 measurements with rHF, its variants, and rLF. The kinetic scheme initially used for HoSF [27] was applied to rHF to predict the Fe^{2+}/O_2 stoichiometry, the steady-state H_2O_2 concentration produced during reaction, and the expected H_2O_2 concentration following completion of the iron deposition reaction.

4.1. Scheme 1

In this sequence of reactions, H_2O_2 is assumed to initially form [21,28] and then completely reacts with a system component designated as X[2] in Reaction 3. Using rate constants reported in Table 1, the assumption that H_2O_2 reacts ~10-fold faster with X than with Fe^{2+} to give Fe^{2+}/O_2 values near 2.0 and the kinetic simulation procedures for HoSF previously reported for Scheme 1, the kinetic behavior shown in Fig. 8 was calculated. The simulation predicts Fe^{2+}/O_2 values of near 2.4 and shows that H_2O_2 rapidly forms, reaches a maximum but narrow steady-state concentration of ~12.0 μM at ~600 ms and then rapidly declines to zero by 10 s as it reacts by Reaction 3. Fig. 8 is consistent with Fig. 3 and with direct H_2O_2 measurements using frog H ferritin [23] obtained as a function of time by freeze quench methods. However, the results in Fig. 8 and the freeze quench studies differ on the time scale for H_2O_2 development, with 70 ms [23] and 600 ms (Fig. 8) being the estimated times of maximum steady-state H_2O_2 production for frog H ferritin and rHF, respectively. This difference may be due to different rates in forming the H_2O_2 precursor by the two different proteins, or if k3 is larger than assumed (20 s^{-1}), then the difference could be attributed to a faster rate for Reaction 3, which moves the peak in Fig. 9 to shorter times for rHF.

The absence of H_2O_2 (Fig. 3) the freeze quench measurements and the simulated results in Fig. 9 are not in accord with two independent reports [16,21] that 30–50%

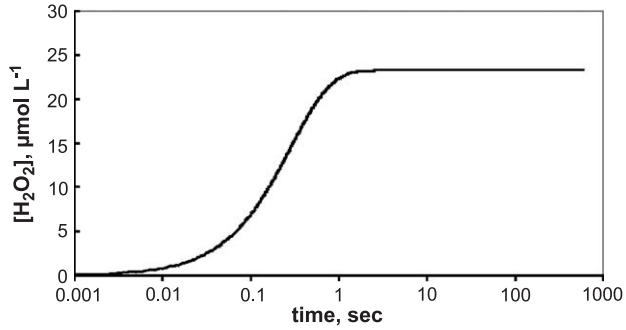

Fig. 9. Simulation of H_2O_2 production using Scheme 3 as a function of time at pH 7.5 and 5.0 μM AvBF at a Fe^{2+}/AvBF ratio of 50 at 210 μM O_2 using the rate constant of 0.34 s^{-1} from Table 1 for both Fe^{2+} oxidation with O_2 and H_2O_2.

[2] X is an unidentified solution component previously postulated [21,28]. X is used only as an illustration to discuss the kinetic and stoichiometric consequences of its reacting with newly formed H_2O_2 because the nature of X is unknown. All oxo transfer reactions leading to aldehydes, ketones, alcohols, acids, N-oxides, and peroxo compounds are consistent with Reaction 3. Reactions such as $X+H_2O_2+H^+=XOH+H_2O$ give H^+/O_2 of 3.0 and H^+/Fe^{2+} of 1.5, not the measured values of 4.0 and 2.0.

$$2\,Fe^{2+} + O_2 + 6H_2O = 2Fe(OH)_3 + H_2O_2 + 4H^+ \qquad (1)$$

$$\underline{\tfrac{1}{2}\,X + \tfrac{1}{2}\,H_2O_2 = \tfrac{1}{2}\,XO + \tfrac{1}{2}\,H_2O} \qquad (3)$$

$$2Fe^{2+} + O_2 + 11/2\,H_2O + \tfrac{1}{2}\,X = 2Fe(OH)_3 + \tfrac{1}{2}\,H_2O_2 + 1/2\,XO + 4\,H^+ \qquad (5)$$

Scheme 2.

of the H_2O_2 predicted by Reaction (1) is destroyed by catalase following the iron deposition reaction. The release of O_2 by catalase, presumably from H_2O_2 released into solution, is extensive, although the assumption is made that all H_2O_2 is consumed in a secondary reaction to give a Fe^{2+}/O_2 value near 2.0. These results are difficult to reconcile, and we explored an alternate reactivity pattern represented by Scheme 2 to explain the release of O_2 by catalase [16,21].

4.2. Scheme 2

To explain O_2 release with catalase, Scheme 2 assumes that only half of the H_2O_2 reacts with *X* and the remainder is released into solution. Reaction 5 correctly predicts Fe^{2+}/O_2 and H^+/Fe^{2+} values of 2.0 and the presence of H_2O_2, in agreement with previous O_2 release measurements. However, such a proposal is not totally satisfying because (1) experiments demonstrating 30–50% formation of H_2O_2 [16,21] and the results reported here and previously [23] showing no H_2O_2 formation after 30 s were conducted under similar conditions, and differences are not expected; (2) It is mechanistically difficult to visualize how Reaction 3 in Scheme 2 only consumes one-half of the H_2O_2; and (3) Scheme 2 requires that H_2O_2 is produced in the presence of unreacted Fe^{2+} and should undergo rapid reaction, as measured in Figs. 2 and 3. This latter consideration is significant because if Fe^{2+} rapidly reacts with released H_2O_2 as shown in Fig. 2, then the Fe^{2+}/O_2 stoichiometry should increase to 3.0, which is not observed. These considerations leave Scheme 2 an incomplete explanation and leave the apparently contradictory results that *all* H_2O_2 reacts with the protein complex and the well-established reactivity pattern of 30–50% H_2O_2 released into solution unexplained and in need of new insights and experimentation to resolve them.

It is interesting that for HoSF, little or no H_2O_2 was observed and all three groups [16,20,21] report Fe^{2+}/O_2 values of 2.0–2.5, indicating that Scheme 1 adequately describes its reactivity. HoSF is heteropolymeric consisting mainly of L subunits (~3 H and ~21 L), and H_2O_2 reacts completely with *X*, whereas, with recombinant H proteins, two different types of reactivity seem to occur, possibly in a conditions-sensitive manner. This behavior led us to consider the reactivity of rLF consisting of all L subunits.

Fig. 4 provides important insight into H_2O_2 formation by the rLF-catalyzed Fe^{2+} oxidation by O_2. It is accepted that the ferroxidase center, found within the H subunit, catalyzes the oxidation of Fe^{2+} by O_2 [1–5] and is the site of H_2O_2 production [14,15,21,23,34,35]. rLF does not contain the ferroxidase center ligands, and the 222 protein has these rHF ligands replaced. In contrast to rHF and its site-altered forms, rLF and 222 only slowly oxidize Fe^{2+} with O_2 to form mineral cores. It is surprising then that rLF gives a Fe^{2+}/O_2 stoichiometry of 2.65, a result that suggest initial H_2O_2 formation in a protein lacking the ferroxidase center. This Fe^{2+}/O_2 value also suggests that the newly formed H_2O_2 reacts in a secondary reaction (Reaction 3 in Scheme 1) because no H_2O_2 is detected (Fig. 3), although a small amount was reported with Amplex Red [28]. Another surprising feature of the rLF reaction is that Fig. 4 shows that H_2O_2 reacts 100–200 times faster with Fe^{2+} than does O_2, hence the newly formed H_2O_2 should readily oxidize Fe^{2+} and give a Fe^{2+}/O_2 ratio of 4.0, if Reaction 3 in Scheme 3 does not occur. However, the formation of H_2O_2 by O_2 reduction is 200-fold slower than for rHF but, importantly, the secondary reaction must out-compete the rapid Fe^{2+} oxidation by H_2O_2 shown in Fig. 4 to give a Fe^{2+}/O_2 value of 2.65. If this is so, then Reaction 3 in Scheme 1 is much faster in rLF than in rHF. It must also be that this secondary reaction occurs at a site other than the ferroxidase center because this is lacking in rLF. Does the H_2O_2 generated by rLF and rHF react with *X* in the same manner in the secondary reaction? If so, where does this reaction occur and what are the products? These questions are currently being investigated.

4.3. AvBF reactions

E. coli and *L. innocua* ferritins produce H_2O from O_2 reduction during the iron deposition reaction [18,19]. With EcBF, H_2O_2 was suggested as an intermediate that was released into solution at an appreciable concentration during both ferroxidation and mineralization reactions but, curiously, in neither case was O_2 released upon catalase addition. These results differ from the reactivity of rHF and other animal ferritins discussed above, where H_2O_2 is an intermediate product but instead of reacting with $2Fe^{2+}$ to give Fe^{2+}/O_2 values of 4.0 as with EcBF, it reacts in a

$$2\,Fe^{2+} + O_2 + 6H_2O = 2Fe(OH)_3 + H_2O_2 + 4H^+ \qquad (1)$$

$$\underline{2\,Fe^{2+} + H_2O_2 + 4H_2O = 2Fe(OH)_3 + 4H^+} \qquad (6)$$

$$4Fe^{2+} + O_2 + 10H_2O + X = 4Fe(OH)_3 + 8H^+ \qquad (7)$$

Scheme 3.

secondary reaction giving Fe^{2+}/O_2 values of 2.0. To explain these differences, it was assumed that H_2O_2 initially formed but the bacterial ferritin ferroxidase centers efficiently use it to oxidize additional Fe^{2+} [18]. It was of interest to determine if AvBF behaved as EcBF to initially form H_2O_2, which rapidly reacted with 2 Fe^{2+} to form H_2O and give Fe^{2+}/O_2 values of 4.0 or to give values of ~2.0 as with the animal ferritins because of a secondary reaction.

Fig. 6 confirms the absence of H_2O_2 formation with AvBF and Fig. 5, and oximetric measurements gave Fe^{2+}/O_2 values near 4.0, demonstrating that O_2 is reduced to H_2O. However, the observation made here that H_2O_2 and O_2 react at the same rate (Table 1) with Fe^{2+} has important implications if H_2O_2 is formed and released into solution. The series of reactions shown in Scheme 3 represents the formation and release of H_2O_2 free into solution, which then reacts with Fe^{2+}.

When this Scheme is combined with the rate constants from Table 1, the simulated behavior shown in Fig. 9 is calculated and shows that H_2O_2 initially forms slowly but after ~1 s has reached a value of 23 μM, which remains constant with time and should be easily measured using Amplex Red. This behavior can be understood because both O_2 and H_2O_2 oxidize Fe^{2+} at nearly identical rates (Table 1), but O_2 is constant at 210 μM, and if the newly formed H_2O_2 is released into solution, its concentration will only approach ~μM concentrations. Because of this concentration differential, the reaction of excess O_2 with Fe^{2+} is faster by a factor of ~200 or more, which causes the predicted build-up of H_2O_2 shown in Fig. 9. That none is measured by Amplex Red (Fig. 6) suggests that Scheme 3 is not a correct description of AvBF reactivity. We conclude that O_2 must be reduced directly to H_2O by $4Fe^{2+}$ without intermediate formation and release of H_2O_2. Such reactivity makes the differences between AvBF and rHF and their quite similar ferroxidase centers quite remarkable!

The behavior of AvBF also stands in contrast to EcBF in several respects. The first-order rate constant of 0.60 s^{-1} for iron deposition with O_2 in EcBF [36] is twice as fast as that reported here for the reaction with AvBF (0.34 s^{-1}). The reaction with H_2O_2 is even more pronounced because EcBF reacts 10 times faster with H_2O_2 than with O_2 [37]. This makes the H_2O_2 reaction for EcBF ~20 times faster than the corresponding reaction with AvBF. From the above kinetic information, the H_2O_2 concentration produced by EcBF as a function of time was simulated and compared to that for AvBF. A curve similar to Fig. 9 was observed, except the H_2O_2 concentration was estimated to be only 2.0–4.0 μM at the end of the reaction instead of 23 μM in Fig. 9 for AvBF. This decrease is due to the 10-fold faster reaction of H_2O_2 with Fe^{2+} for EcBF compared to AvBF. However, the simulation for H_2O_2 production for EcBF must be considered only approximate for two reasons: (1) the EcBF rate data were for pH 6.5 and that for AvBF was for pH 7.5, and pH does affect the rate as reported earlier; and (2) the 10-fold faster rate for H_2O_2 compared to O_2 for EcBF was not calculated from precise kinetic fitting but by relative measurements [37]. Nevertheless, for EcBF, the prediction of H_2O_2 formation from the simulation is consistent with measurements of H_2O_2 during iron deposition [37] and suggests that some H_2O_2 is formed and released during EcBF iron deposition but reacts with Fe^{2+} as proposed [37]. AvBF is unique in that if H_2O_2 is an intermediate, it is not released into solution but is apparently reduced *in situ* to H_2O. This reactivity difference is of interest and may imply the involvement of the heme groups in H_2O_2 reactivity because the AvBF used here was native and contained 12 heme groups [33], whereas the EcBF protein was prepared by recombinant methods and had a 10-fold lower heme content of only 1.3 heme/EcBF. The reduction of O_2 to H_2O by AvBF and the intermediate formation and release of H_2O_2 by EcBF may be a consequence of the differences in heme content.

4.4. The secondary reaction

Attempts to address the nature of Reaction 3 have focused on the reaction of added H_2O_2 toward apo and holo ferritins. The observations that apo HoSF and rHF and their holo forms only slowly react with externally added H_2O_2 in a catalase type-reaction [20–22] are in accord with results reported here. However, the slowness of this reaction (~1 h) is not compatible with Reaction 3, which occurs within milliseconds, leaving the experiments with externally added H_2O_2 an unlikely explanation for Reaction 3. The identity of *X* and the question of where its reaction with H_2O_2 occurs on the protein and what is the product of *X* oxidation remain unknown and our efforts are being directed more to the possibility that *X* is a buffer component, a possibility which needs greater scrutiny[3].

Acknowledgement

This research was partially supported by the Undergraduate Research Program of the College of Mathematics and Physical Science at Brigham Young University.

References

[1] P.M. Proulx-Curry, N.D. Chasteen, Molecular aspects of iron uptake and storage in ferritin, Coord. Chem. Rev. 144 (1995) 347–368.
[2] G.S. Waldo, E.C. Theil, Ferritin and iron biomineralization, in: K.S. Suslick (Ed.), Comprehensive Supramolecular Chemistry, vol. 5, Pergamon Press, Oxford, U.K., 1996, pp. 65–89.
[3] P.M. Harrison, P. Arosio, The ferritins: molecular properties, iron storage function and cellular regulation, Biochim. Biophys. Acta 1275 (1996) 161–203.

[3] In separate unpublished observations, we have found that as the Mops concentration decreases, the Fe^{2+}/O_2 ratio increases. This result, kinetic simulations and other results to be published later suggest that Mops may be the component *X* in Scheme 1.

[4] E.C. Theil, Ferritin structure gene regulation and cellular functionin animals, plants and microorganisms, Annu. Rev. Biochem. 56 (1987) 289–316.
[5] N.D. Chasteen, P.M. Harrison, Mineralization in ferritin: an efficient means of iron storage, J. Struct. Biol. 126 (1999) 182–194.
[6] A. Treffry, P.M. Harrison, Incorporation and release of inorganic phosphate in horse spleen ferritin, Biochem. J. 171 (1978) 313–320.
[7] J.L. Johnson, M. Cannon, R.K. Watt, R.B. Frankel, G.D. Watt, Forming the phosphate layer in reconstituted horse spleen ferritin and the role of phosphate in promoting core surface redox reactions, Biochemistry 38 (1999) 6706–6713.
[8] G.D. Watt, R.B. Frankel, D. Jacobs, H. Huang, G.C. Papaefthymiou, Fe^{2+} and phosphate interactions in bacterial ferritin from *Azotobacter vinelandii* bacterial ferritin, Biochemistry 31 (1992) 5672–5679.
[9] J.S. Rohrer, Q.T. Islam, G.D. Watt, D.E. Sayers, E.C. Theil, Iron environment in ferritin with large amounts of phosphate from *Azotobacter vinelandii* and horse spleen, analyzed using extended X-ray absorption fine structure (EXAFS), Biochemistry 29 (1990) 259–264.
[10] S. Andrews, Iron storage in bacteria, Adv. Microb. Physiol. 40 (1998) 282351.
[11] D.M. Lawson, A. Treffry, A.P.J. Artymiuk, P.M. Harrison, P.M.S.J. Yewdall, A. Luzzago, G. Cesareni, S. Levi, P. Arosio, Identification of the ferroxidase center in ferritin, FEBS Lett. 254 (1989) 207–210.
[12] P.D. Hempsted, A.J. Hudson, P.J. Artymiuk, S.C. Andrews, M.J. Banfield, J.R. Guest, P.M. Harrison, Direct observation of the iron binding sites in a ferritin, FEBS Lett. (1994) 258–262.
[13] S. Levi, A. Luzzago, G. Cesareni, A. Cozzi, F. Franceschenelli, A. Albertini, P. Arosio, Mechanism of ferritin iron uptake: activity of the H-chain and deletion mapping of the ferro-oxidase site, J. Biol Chem. 263 (1988) 18086–18092.
[14] B. Xu, N.D. Chasteen, Iron oxidation chemistry in ferritin. Increasing Fe/O2 stoichiometry during core formation, Biol. Chem. 266 (1991) 19965–19970.
[15] S. Sun, P. Arosio, S. Levi, N.D. Chasteen, Ferroxidase kinetics of human liver apoferritin recombinant H-chain apoferritin and site-directed mutants, Biochemistry 32 (1993) 9362–9369.
[16] G.S. Waldo, E.C. Theil, Formation of iron (III)-tyrosinate is the fastest reaction observed in ferritin, Biochemistry 32 (1993) 13262–13269.
[17] X. Yang, Y. Chen-Barrett, P. Arosio, N.D. Chasteen, Reaction paths of iron oxidation and hydrolysis in horse spleen and recombinant human ferritins, Biochemistry 37 (1998) 9743–9750.
[18] X. Yang, N.E. Le Brun, A.J. Thomson, G.R. Moore, N.D. Chasteen, The iron oxidation and hydrolysis chemistry of *Escherichia coli* bacterioferritin, Biochemistry 39 (2000) 4915–4923.
[19] X. Yang, E. Chiancone, S. Stefanini, A. Ilari, N.D. Chasteen, Iron oxidation and hydrolysis reactions of a novel ferritin from *Listeria innocua*, Biochem. J. 349 (2000) 783–786.
[20] S. Lindsay, D. Brosnahan, G.D. Watt, Hydrogen peroxide formation during iron deposition in horse spleen ferritin using O2 as an oxidant, Biochemistry 40 (2001) 3340–3347.
[21] G. Zhao, F. Bou-Abdallah, X. Yang, P. Arosio, N.D. Chasteen, Is hydrogen peroxide produced during iron (II) oxidation in mammalian apoferritins? Biochemistry 40 (2001) 10832–10838.
[22] D.E. Mayer, J.S. Rohrer, D.A. Schoeller, D.C. Harris, Fate of oxygen during ferritin iron incorporation, Biochemistry 22 (1983) 876–880.
[23] G.N.L. Jameson, W. Jin, C. Krebs, A.S. Perreira, P. Tavares, X. Liu, E.C. Theil, B.H. Huynh, Stoichiometric production of hydrogen peroxide and parallel formation of ferric multimers through decay of the diferric–peroxo complex, the first detectable intermediate in ferritin mineralization, Biochemistry 41 (2002) 13435–13443.
[24] A. Treffry, Z. Zhao, M.A. Quail, J.R. Guest, P.M. Harrison, Iron (II) oxidation by H chain ferritin: evidence from site-directed mutagenesis that a transient blue species is formed at the dinuclear iron center, Biochemistry 34 (1995) 15204–15213.
[25] F. Bou-Abdallah, G.C. Papaefthymiou, D.M. Scheswohl, S.D. Stanga, P. Arosio, N.D. Chasteen, μ-1,2-Peroxobridged di-iron (III) dimer formation in human H-chain ferritin, Biochem. J. 363 (2002) 57–63.
[26] S. Lindsay, D. Brosnahan, T.J. Lowery Jr., K. Crawford, G.D. Watt, Kinetic studies of iron deposition in horse spleen ferritin using O2 as oxidant, Biochim. Biophys. Acta 1621 (2003) 57–66.
[27] T.J. Lowery, J. Bunker, B. Zhang, R. Costen, G.D. Watt, Kinetic studies of iron deposition in horse spleen ferritin using O_2 and H_2O_2 as oxidant, Biophys. Chem. 111 (2004) 173–181.
[28] G. Zhao, F. Bou-Abdallah, P. Arosio, S. Sevi, C. Janus-Chandler, N.D. Chasteen, Multiple pathways for mineral core formation in mammalian apoferritin. The role of hydrogen peroxide, Biochemistry 42 (2003) 3142–3150.
[29] S. Levi, G. Cesareni, P. Arosio, R. Lorenzetti, M. Soria, M. Sollazzo, A. Albertini, R. Cortese, Characterization of human ferritin H chain synthesized in *Escherichia coli*, Gene 51 (1987) 267–272.
[30] S. Levi, J. Salfeld, F. Franceschinelli, A. Cozzi, M.H. Dorner, P. Arosio, Expression and structural and functional properties of human ferritin L-chain from *Escherichia Coli*, Biochemistry 28 (1989) 5179–5184.
[31] J.l. Johnson, D.C. Norcross, P. Arosio, R.B. Frankel, G.D. Watt, Redox reactivity of animal apoferritins and apoheteropolymers assembled from recombinant heavy and light human chain ferritins, Biochemistry 38 (1999) 4089–4096.
[32] E.E. Stiefel, G.D. Watt, Azotobacter cytochrome $b_{557.5}$ is a bacterioferritin, Nature 279 (1979) 81–83.
[33] G.D. Watt, J.W. McDonald, C.-H. Chiu, K.R.N. Reddy, Further characterization of the redox and spectroscopic properties of *Azotobacter vinelandii* ferritin, J. Inorg. Biochem. 5 (1) (1993) 745–758.
[34] P. Moenne-Loccoz, C. Krebs, K. Herlihy, D.E. Edmondson, E.C. Theil, B.H. Huynh, T.M. Loehr, The ferroxidase reaction of ferritin reveals a diferric μ-1, 2 bridging peroxide intermediate in common with other O_2-activating non-heme diiron proteins, Biochemistry 38 (1999) 5290–5295.
[35] A. Pereira, W. Small, C. Krebs, P. Tavares, D. Edmondson, E. Theil, B. Huynh, Direct spectroscopic and kinetic evidence for the involvement of a peroxodiferric intermediate during the ferroxidase reaction in fast ferritin mineralization, Biochemistry 37 (1998) 9871–9876.
[36] H. Aitken-Rogers, C. Singleton, A. Lewin, A. Taylor-Gee, G.R. Moore, N.E. Le Brun, Effect of phosphate on bacterioferritin-catalyzed iron (II) oxidation, J. Biol. Inorg. Chem. 9 (2004) 161–170.
[37] F. Bou-Abdallah, A.C. Lewin, N.E. Le Brun, G.R. Moore, N.D. Chasteen, Iron detoxification properties of *Escherichia coli* bacterioferritin, J. Biol. Chem. 277 (2002) 37064–37069.